Editorial Manager(tm) for Meteorology and Atmospheric Physics
Manuscript Draft

Manuscript Number: MAP-D-06-00073

Title: The twelve most intense cold surges in southeastern Brazil in the period 1979-2005

Article Type: Original Paper

Keywords:

Corresponding Author: prakki satyamurty, Ph. D.

Corresponding Author's Institution: Instituto Nacional de Pesquisas Espaciais (INPE)

First Author: Prakki Satyamurty, Ph. D.

Order of Authors: Prakki Satyamurty, Ph. D.; Luiz Fernando de Mattos, Ph. D.; prakki satyamurty, Ph. D.

Abstract: The characteristics of potential vorticity (PV), frontogenetic function (FF) and other diagnostic fields associated with the twelve most intense cold surges in southeastern Brazil in the period 1979-2005 for up to seven days before the events are presented. They reveal many interesting common features, thus permitting the construction of composite fields representative of the events. The development and east-northeastward progression (~ 6.5° longitude per day) of mid-latitude baroclinic perturbations responsible for the cold surges and the associated surface and upper air flow features during the 7-day period are described. A surface high-pressure center, after crossing the Andes in southern Chile, progresses rapidly to the region around Paraguay on days -2 and -1. A surface low in the Atlantic off Argentina moves slowly southeastward. On day -1 meridional winds east of the surface high, with a large fetch, advect cold air into southeastern and central Brazil causing the cold surges. A wave train intensification with a southwest to northeast orientation in the region around southern South America is clearly seen in the 250-hPa meridional wind component from days -4 to -1. The frontogenesis function in the lower troposphere (925 and 850 hPa levels) and the 325°K isentropic potential vorticity fields show significant signals of development in the three days before the events. The anomaly fields indicate the evolution of the strong cold surges with longer lead times than the whole fields. A good monitoring of the diagnostics can signal the occurrence of the very strong cold surges in southeastern Brazil with lead times of the order of 72 hours.

The twelve most intense cold surges in southeastern Brazil in the period 1979-2005

By

Luiz Fernando de Mattos and Prakki Satyamurty

Centro de Previsão de Tempo e Estudos Climáticos (CPTEC) – Instituto Nacional de Pesquisas Espaciais (INPE) – São José dos Campos – SP – Brazil

November 2006

Abstract

The characteristics of potential vorticity (PV), frontogenetic function (FF) and other diagnostic fields associated with the twelve most intense cold surges in southeastern Brazil in the period 1979-2005 for up to seven days before the events are presented. They reveal many interesting common features, thus permitting the construction of composite fields representative of the events. The development and east-northeastward progression (~ 6.5° longitude per day) of mid-latitude baroclinic perturbations responsible for the cold surges and the associated surface and upper air flow features during the 7-day period are described. A surface high-pressure center, after crossing the Andes in southern Chile, progresses rapidly to the region around Paraguay on days –2 and –1. A surface low in the Atlantic off Argentina moves slowly southeastward. On day –1 meridional winds east of the surface high, with a large fetch, advect cold air into southeastern and central Brazil causing the cold surges. A wave train intensification with a southwest to northeast orientation in the region around southern South America is clearly seen in the 250-hPa meridional wind component from days –4 to –1. The frontogenesis function in the lower troposphere (925 and 850 hPa levels) and the 325°K isentropic potential vorticity fields show significant signals of development in the three days before the events. The anomaly fields indicate the evolution of the strong cold surges with longer lead times than the whole fields. A good monitoring of the diagnostics can signal the occurrence of the very strong cold surges in southeastern Brazil with lead times of the order of 72 hours.

1. Introduction

Cold frontal passages in southern and southeastern Brazil followed by cold air incursions are very common meteorological events in winter half of the year (Satyamurty et al. 1998). According to the Centro de Previsão de Tempo e Estudos Climáticos (CPTEC) enumeration reported in the monthly summaries in "Climanálise" two to three episodes per month on the average are expected from May through September. The cold air incursions bring discomfort to the society. Health problems, especially respiratory ailments, increase during these months in southeastern and southern regions of Brazil. Some strong cold air incursions are responsible for the occurrence of frost that can inflict substantial loss to the agriculture and horticulture sectors in southeastern Brazil (Marengo et al. 1997, Satyamurty et al. 2002), especially in the states of São Paulo and southern Minas Gerais (see locator map in Fig. 1). Reliable prediction and monitoring of these meteorological events, especially the very strong ones, is an important forecasting issue in Brazil.

Several meteorological aspects of the cold surges in Brazil are studied by Kousky (1979), Fortune and Kousky (1983), Marengo et al. (1997), Krishnamurti et al. (1999), Lupo et al. (2001), Satyamurty et al. (2002), Pezza and Ambrizzi (2005) and Muller et al. (2005). Garreaud (2000), Vera and Vigliarolo (2000), Vera et al. (2002) and Muller et al. (2003) also noted several characteristics of these events in southern and subtropical South America. These studies revealed the following general characteristics: (1) The cold fronts approaching from the south occasionally penetrate deep into the continent of South America as far north as 10°S or beyond. (2) The cold frontal passages over South America are associated with developing baroclinic waves in the westerlies, which are influenced by

the Andes topography. (3) A high pressure center over Argentina along with the development of a trough or a cyclone in the Atlantic off the Argentina coast drive strong cold southerly winds over the east coast of Argentina and deep into Brazil causing cold surges in central and northern Brazil.

Pezza and Ambrizzi (2005) have calculated atmospheric variables and the cyclone and anticyclone tracks at the surface from day –10 to day 0 with regard to the coldest day in São Paulo. They have categorized the cold waves into extreme, strong and moderate and have found that most of the cold events in São Paulo can be tracked up to nine days before the occurrence.

However, none of the above mentioned studies have examined the events from the points of view of isentropic potential vorticity and frontogenetic function, which is undertaken here. Our intention is also to reexamine the evolution of the synoptic features up to 7 days prior to the very strong cold surges in southeastern Brazil. The present study focuses on the characterization of the associated upper and lower tropospheric flow patterns. The identification of the most intense cold surges in southeastern Brazil is based on the minimum temperature registered at the Instituto Astrofísico e Geofísico/Universidade de São Paulo (IAG/USP) meteorological station (Fig. 1).

Special attention is paid to the cold surges in São Paulo because the cold surge events in southern South America (Chile and Argentina) and in southeastern Brazil are not necessarily related. To verify this we have compared the cases of generalized frost in the wet Pampa region in northern Argentina reported by Muller and Berri (2006) and the cases

of cold surges in São Paulo reported by Pezza and Ambrizzi (2005). Except for one case in which wet Pampa reported frost on 18 June 1981 and two days later São Paulo reported strong frost, all other cases during the 30-year period 1961-1990 were different in the two regions.

2. Data and Methodology

The daily minimum temperature data at IAG/USP meteorological station for the period 1979 through 2005 is used to identify the very strong cold surges in southeastern Brazil. For obtaining a threshold value for defining the very strong cold surges the frequency distribution of the daily minimum temperatures (Tmin) observed on the 4131 days in the months of MJJAS is used. There are 0,4 % of the days (16 days) with Tmin values less than 3°C. These days are identified. The dates reveal that 12 of them are the beginning days of distinct cold surge events. During a sequence of consecutive days with Tmin < 3°C the first day is considered as the beginning of the event. These 12 days, one for each separate event, are designated as D0 or day 0. On nine D0s frost was reported at the meteorological station.

The D0 composite fields for the atmospheric variables and other diagnostics are obtained by taking an average over the 12 cases for day 0 at 12 UTC (corresponds to 09 LT). Similarly composites for the days -1, -2, …, -7 prior to D0, designated D-1, D-2, .. D-7, respectively, are obtained by averaging the fields for the corresponding 12 days. The anomaly fields are obtained both for the individual cases and for the composites by subtracting the month's climatological field.

The NCEP/NCAR reanalysis (Kalnay et al. 1996) data sets for the four synoptic hours are used to prepare the charts for the atmospheric variables and the diagnostics thereof to study the characteristics before and during the strong cold surge events. The variables and the derived diagnostics used in this study are: wind (**V**(u, v)), temperature (T), potential temperature (θ), surface pressure (p_s), geopotential (ϕ), relative vorticity (ζ), Rossby´s potential vorticity (PV) and Petterssen's frontogenetic function (FF) (Bluestein 1993). The last two diagnostics are given by

$$PV = - g (\partial\theta/\partial p)(\zeta + f) \quad (1)$$

$$FF = |\nabla\theta|(D \cos\gamma - \delta) \quad (2)$$

where f is the Coriolis parameter, D is the net deformation, γ is the angle between the dilatation axis and the thermal gradient and δ is horizontal divergence. For further details on how FF is calculated see Satyamurty and Mattos (1989).

The potential vorticity on an isentropic surface in the upper tropospheric levels is a very well studied diagnostic for the synoptic perturbation development (Hoskins et al. 1985, Davis and Emanuel 1991, Montgomery and Farrel 1991, Davies and Rossa 1998, Bluestein 1993, Nielson-Gammont 2001). Here, the PV fields on the 325°K isentropic surface and their composites and anomalies are used.

The cold surges are all associated with cold frontal passages. The formation, intensification and movement of the fronts associated with the baroclinic wave development can be diagnosed with the help of frontogenesis function. There are many mechanisms responsible for frontogenesis (Hoskins and Brotherton 1972). However, a scale analysis of the different mechanisms (terms) of frontogenesis in the lower troposphere (considering that the synoptic scale vertical motions are small near the surface) shows that the most important mechanisms are the actions of confluence and convergence on preexisting baroclinic zones. These effects are represented in the expression for FF (Eq. 2). In the present study FF is calculated at 925 and 850 hPa levels.

3. Trajectories of Pressure Centers

The trajectories of the high- and low-pressure centers during the 7-day period prior to the events of strong cold surges in southeastern Brazil are drawn by following the surface pressure analyses at intervals of 12 hours in the twelve cases considered in this study and are shown in Fig. 2. When there is no well-defined or closed low-pressure center in the isobaric analysis east of the high-pressure center, the anomaly field is examined to draw the trajectory of the low center. The trajectories obtained here agree fairly well with the portion of the pressure center tracks around the South American continent shown in Pezza and Ambrizzi (2005) except that the trajectories in these 12 cases are limited to 100°W – 30°W. The high-pressure centers have their origin in the eastern South Pacific off the Chile coast and move southeastward in the ocean. On D-2 they enter the continent through southern Chile and, after crossing the Andes, move northward to northern Argentina north of 30°S on D-1. On D0 they are located in southern Brazil and adjoining

regions of Argentina and Uruguay. The low-pressure centers or troughs originate in the northernmost regions of Argentina and move southeastward rapidly into the South Atlantic south of 30°S. On D-2, D-1 and D0 they move further to southeast in the Atlantic between 35°S and 50°S. On D-2 and D-1 the high center moves rapidly northeastward and the low center moves slowly. As a result the distance between the high and low centers diminish which helps to build the pressure gradient necessary for strengthening southerly winds in the lower troposphere. The cold winds with a large fetch are responsible for the cold surges in the central and northern parts of Brazil, as was earlier explained by many authors (ex. Satyamurty et al. 2002).

4. Surface Pressure, Temperature, Geopotential, Thickness and Upper Wind Patterns

The surface pressure fields in the 12 cases, their composites and the composite anomalies along with the winter climatology for D0 and D-1 are shown in Figs. 3 and 4, respectively. It is interesting to note that there are many similarities among the individual cases (Fig 3 a-l) on D0, principal similarities being the high-pressure center in Argentina and the trough in South Atlantic. These similarities justify and validate the representativeness of the composite field (Fig. 3 n). The spatial correlation coefficient values between the anomalies of the individual cases and the composite anomalies are all very high, exceeding 0.9 in many cases both on D0 and D-1. This suggests that the very strong cold surges in São Paulo are caused by synoptic disturbances having the same pattern.

The high center on D-1 in northern Argentina is stronger than 1024 hPa which somewhat weakens on D0. The trough or low-pressure center in the Atlantic is 1008 hPa. In the composite anomaly fields on D0 and D-1 (Fig. 3 o and Fig. 4 o) the positive anomaly over Argentina is 10 hPa and the negative anomaly over the South Atlantic is 5 hPa. On D0 the high-pressure anomaly shows an important northward penetration over the continent, east of the Andes. The trough in the South Atlantic Ocean is associated with a frontal boundary extending into the continent around 20°S.

The 1000-500 hPa thickness composites are superposed on the pressure composites (Fig. 3 n and Fig. 4 n). It is interesting to note that the cold air (thickness trough) is located to the west of the Atlantic trough. On D0 the thickness trough somewhat weakens and moves eastward on to southern and southeastern Brazil. It is to be remembered that the minimum temperature below 3°C in São Paulo is observed around 09 UTC, three hours before the hour of the field on D0 (12 UTC). Thus, the advective cooling that is indicated in the D-1 pressure and temperature field (Fig. 4 n), besides the nocturnal cooling, is important for the temperature fall. The surface pressure patterns and their composites for D-2 and D-3 (figures not given) also show many common features among the 12 cases.

The composites for the days D-7, D-5, D-4, D-3, D-2, D-1 and D0 and their anomalies for p_s are given in Fig. 5. The areas where the anomalies are statistically significant at 95% level are shaded. The positive anomaly west of Chile becomes significant on D-5 and the low-pressure anomaly in the South Atlantic is significant since D-4. The positive anomaly gradually moves on to the continent during the following three

days. On D-1 it is significant over Argentina and on D0 over the region around Paraguay. The 1000-500 hPa thickness trough, which indicates the cold air mass, on D-4 through D0, is to the west of the Atlantic trough that coincides with the frontal boundary at the surface (Figs. 5 e, g, i, k, m). The 850-hPa temperature composites and their anomalies for the same lead times are shown in Fig. 6. The temperature trough over the continent, which coincides with the thickness trough (Fig. 5), gains amplitude from D-3 and its anomaly in southern Brazil increases from –3°C on D-4 to –6°C on D-1. It is important to remember that the anomalies in individual cases are always stronger than in the composites and that the temperature differences are larger at the surface than at 850 hPa.

Figure 7 shows the 500-hPa geopotential composites and their anomalies for D-7, D-5, D-4, D-3, D-2, D-1 and D0. A wave pattern in the composites is evident from D-4 onward (Figs. 7 e, g, i, k, m) which progresses eastward at a speed of approximately 6.5° longitude per day, as can be seen from the trough positions at 30°S on D-4 and D0. In the middle latitudes the positive anomaly at the ridge on D-4 is 100 m and negative anomaly at the trough is 50 m. As the wave intensifies, the negative anomaly at the trough deepens to 150 m over southern Brazil on D-1, indicative of the advection of cold air mass in the lower troposphere. The northward component of propagation of the 500-hPa trough, more easily seen in the anomaly fields (Fig. 7 f, h, j, l), is important for the cold surges in central Brazil.

The midlatitude troughs and ridges and cyclonic and anticyclonic regions in the upper troposphere can be followed by analyzing the meridional wind component (v) fields at, say, 250-hPa level. Fig. 8 presents the v composites and their anomalies from D-7

through D0. In this field also, as in 500-hPa geopotential field, a wave train pattern of positive and negative values of v and its anomalies can be seen in the longitude belt of 150°W to 30°W. With the help of the spatial correlations for lags of –3 days up to +3 days in the upper tropospheric streamfunction field, Ambrizzi et al. (1995) noted that there is a strong synoptic wave pattern around south-central South America in austral winter (June-August), indicating teleconnectivity in the region (their figure 3). Additional insight is obtained here by following the patterns for lags of D-7 through D0. Clearly, the amplitude of the wave pattern increases from D-7 till D-2 and then, although remains strong, somewhat weakens on D-1 and D0. Of particular interest are the north wind anomaly in east South Pacific off the Chile coast, south wind anomaly over Argentina and Chile and north wind anomaly over eastern Brazil on D-2. This pattern moves about 12° longitude to the east by D0. The orientation of the arrangement of anomaly maxima and minima is SW-NE in the sector between 180°W and 0°W, whereas it is more east-west in the study of Ambrizzi et al. (1995) for D-3. The wave pattern in the upper tropospheric winds, which can be seen in the whole fields from D-4 through D0 to move with a meridional component of propagation, is associated with strong cold surges in southeastern Brazil. That is, the synoptic wave responsible for strong cold surges up to São Paulo state in SA clearly shows a reasonable northward component of propagation in the middle and upper troposphere. The meridional wind field is appropriate for observing the synoptic wave pattern because the whole v field has almost the same characteristics as its anomaly field (Fig. 8).

It is interesting to observe that all the composite fields discussed so far indicate significant deviations over the continent from their climatological values with lead times of

three to five days. Thus the very strong cold surges in southeastern Brazil are not sudden or surprise events and proper monitoring work can signal their occurrence with reasonable lead time.

5. Diagnostics

a. Frontogenesis function

Supposing that the very strong cold surges in southeastern Brazil are mainly caused by advective affects or frontal movement, the Pettersson's frontogenetic function (FF), which takes into account the horizontal temperature gradients and the wind fields at an appropriate lower level, is a good indicator of the intensification and movement of baroclinic zones. In order to track the baroclinic zones in the lower troposphere FF is calculated at 925 hPa and 850 hPa levels. (Due to terrain irregularities the FF field at the surface becomes very noisy.) The fields at the two levels (850 hPa and 925 hPa) are observed to be very similar and therefore only the 925 hPa composite and anomaly fields for D-7 through D0 are presented here (Fig. 9).

On D-7 a frontogenetic region around Paraguay, extending into southern Brazil and the adjoining Atlantic, is observed. This region is known to be climatologically frontogenetic (Satyamurty and Mattos 1989). The frontogenesis over this region weakens and disappears on D-5. From D-3 onward a frontogenetic region is observed in southern Brazil, which becomes intense on D-2 and D-1, moving into southeastern and eastern Brazil. On D0 the frontogenetic region northward of São Paulo state and frontolytic region in Argentina, southern Brazil and Paraguay are distinctly seen and are strong. The frontogenesis function and the Q vectors are related (Bluestein 1993) such that there is

subsidence over the frontolytic region and ascending motion over the frontogenetic region. Although the subsidence causes warming through adiabatic heating, the advective affects overwhelm the subsidence affect to cause fall of temperature in the lower troposphere in the wake of the frontal boundary. An elongated band of frontogenesis is seen to progress in northeasterly direction from D-4 to D0 (Figs. 9 e, g, i, k, m) at an average speed of 300 km day^{-1} from Paraguay to southern Minas Gerais in four days. On the whole the patterns of frontogenesis and frontolysis regions are also suggestive of the synoptic wave patterns observed in the middle and upper troposphere.

b. Potential vorticity

The potential vorticity (PV) on the 325°K isentropic surface is a good indicator of the lowering of the dynamic tropopause associated with baroclinic waves. (The lowering is due to the advection of the tropopause by strong subsidence in the stratosphere.) Figure 10 presents the PV fields and the corresponding anomaly composites for D-7 through D0. In the whole fields the wave amplification is observed from almost D-5. The anomaly fields show negative values (cyclonic in the Southern Hemisphere) over Argentina on D-4, which become amplified in the following days and move east-northeastward. One important observation is that the cyclonic anomaly forms over Argentina and there is no indication of its migration from the Pacific. Krishnamurti et al. (1999) have identified the progression of PV disturbances from central South Pacific into eastern South America associated with cold surges in southern Brazil, which is not verified in the PV field in the seven days before the strong cold surges in São Paulo. That is, although the wave pattern observed in the

meridional wind shows teleconnectivity between the Pacific and the South American continent, the PV anomaly becomes significant only on D-3 and over Argentina.

The potential vorticity fields on D0 for the 12 cases and their composite are shown in Fig. 11. All the fields are reasonably similar and therefore show strong special correlation with their composite field. The correlation coefficients are 0.7 or larger in most cases. The main features are a trough over Uruguay, Paraguay and southern Brazil and a ridge over southern Argentina and Chile. It is interesting to note that the PV fields are similar to the fields shown in Nielson-Gammon (2001) for the Northern Hemisphere except that the values are negative.

A cyclonic PV anomaly in the upper troposphere embedded in a westerly current increasing with height induces cyclonic development in the lower levels right below the anomaly (Bluestein 1993). The effect at the surface is stronger for stronger and larger scale PV perturbations for a given mean static stability parameter. Figures 10 shows that the PV perturbation over the South American continent is of the synoptic scale and is strong (~ -30 PVU) from D-3. The cyclone at the surface advects cold air west of the center of the anomaly and warm air east of the center of the anomaly in the lower levels. That is, the development of a synoptic scale cyclonic PV anomaly in the upper troposphere supports and strengthens cold advection at the surface west of the center of the anomaly. On D-1 and D0 we find a strong PV anomaly over the region around Uruguay and the adjacent sea in the Atlantic, which supports strong cold advection over the southeastern parts of Brazil. The same characteristics are seen in the individual fields shown in Fig. 11.

6. Independent Case Study

Individual cases are able to provide the true intensity of the diagnostics, which appear smooth in the composite fields. The case of a more recent strong cold surge in São Paulo on 26 July 2005, independent from the composites shown so far, is presented in Figs. 12 – 17. The evolution of the surface pressure and 500-hPa geopotential anomalies and the 925-hPa FF and 325ºK PV and their anomalies are shown with the help of the fields for 168, 144, 120, 96, 84, 72, 60, 48, 36, 24, 18, 12, 06 and 0 hours before the event. The winter (JJA) climatology fields of the surface pressure and geopotential are also given in Figs. 12 and 13. For the FF and PV the climatological fields are presented for the July month only, because these fields were not readily available and are prepared during this study using the reanalyses for 1961-2000. The evolution of this strong cold surge in Southeast Brazil can be better appreciated in the four days preceding the event through the fields at intervals of 12 hours and 6 hours.

The high-pressure anomaly over northern Argentina started building from 96 hours before the cold surge in São Paulo and attained a value of 10 hPa 24 hours before the cold surge (Fig. 12). The low pressure in the Argentina coast started deepening 36 hours before the surge and the anomaly attained a value of 15 hPa 18 hours before the event. These characteristics are seen in the composites for 12 cases but with smaller anomaly values. The 500-hPa negative anomaly (Fig. 13) traveled from the Pacific from 168 hours before the surge to Atlantic during the 7-day period at an average speed of 7° longitude per day which is approximately same as the speed in the composites. However, its deepening was

observed only from 72 hours before the surge. The negative anomaly in the trough one day before the surge was 150 geopotential meters over southern Brazil.

In general, the frontogenesis function (Fig. 14) shows banded structure with a NW-SE orientation, which is expected because the regions favorable for frontogenesis lie along the diffluence lines between the two subtropical high-pressure centers in the two oceans on either side of the continent. The frontogenesis region over Paraguay appeared as early as 108 hours before the surge in São Paulo. This region was organized into a long band and moved slowly northeastward, reacing north of 25°S over the continent by 36 hours before the surge. The frontogenesis weakened over the continent afterwards. The frontolysis over Argentina became strong 18 hours before the event. The same characteristics are evident in the fields of FF anomaly shown in Fig. 15 also. The anomalies, especially those over the central parts of South America, are significant.

The 325°K PV fields are shown in Fig. 16 and its anomaly fields in Fig. 17. Strong cyclonic PV values (PV < -20 PVU) started building up in Argentina 108 hours before the surge in São Paulo. By 60 hours before the surge there was concentration of PV stronger than –40 PVU in northeastern Argentina and neighboring regions. This region moved slowly eastward till 18 hours before the surge. Then on the PV weakened over the continent. The anomalies (Fig. 17) show these characteristics (strengthening of the perturbations and movement) more clearly.

7. Summary

Cold surges over southern and central parts of South America are described in many earlier studies mentioned in the introductory section. The focus of the present study is on the strongest 12 surges in southeastern Brazil (around São Paulo) observed in the 26-year period 1979-2005. This study is important because the southeastern Brazil surges (Pezza and Ambrizzi 2005) and the northern Argentina frost events (Muller and Berri 2006) are found to be mostly unrelated.

The evolution of the atmospheric flow, temperature and pressure patterns associated with these rare 12 strongest cold surge events are presented and discussed. The patterns of evolution in the 12 cases are found to be essentially similar to each other, thus permitting us to form composite fields. A recent independent case of a strong cold surge observed on 26 July 2005 is found to agree satisfactorily with the composites. Lower tropospheric frontogenesis function and 325ºK potential vorticity fields are seen to be useful diagnostic aids for monitoring the subtropical cold surges. Both the composite PV fields and the individual fields show cyclonic PV anomalies in the upper troposphere with sufficient lead time (~ 72 hours), which explain the surface development that follows.

The pressure center trajectories and other atmospheric characteristics showed eastward movement only in the South American region and the adjoining seas in the 7-day period preceding the events. A high-pressure center develops east of the Andes 2 days before the event and moves north-northeastward into Paraguay and southern Brazil region. A low-pressure center or a trough develops in northern Argentina and moves southeastward into the Atlantic. A strong east-west pressure gradient builds on D-1 and the resulting southerly cold winds penetrate the central and southeastern parts of Brazil. The surface

pressure and wind pattern evolution is associated with a developing baroclinic wave, which shows a discernible meridional component of movement.

The results of the present study that can be profitably used in monitoring and prediction of strong cold surges in southeastern Brazil (the region around São Paulo) are summarized below:

i. The strong cold surges in southeastern Brazil are mostly unrelated to the generalized frost events in Northern Argentina.

ii. A baroclinic wave development is observed in the 500-hPa geopotential fields in the period D-3 through D0.

iii. A wave train in the meridional wind component (v) at 250-hPa level becomes evident since D-4.

iv. The evolution and progression of surface high-pressure center and a downstream trough or low, associated with the surges, are observed east of 100°W in the 7-day period before the surges. However, the cold high pressure cell responsible for the cold surge develops east of the Andes on D-2 in central West Argentina and rapidly moves to Paraguay region on D-1 and to southern Brazil on D0.

v. Both the waves at 500-hPa and 250-hPa show a discernible meridional component of propagation to the lower latitudes from D-4.

vi. The anomaly fields are better indicators of the evolution with longer lead times than the whole fields.

vii. The lower tropospheric frontogenesis function (FF) and the 325ºK PV fields and their anomalies are good diagnostics of the evolution of the synoptic disturbance associated with the events.

REFERENCES

Ambrizzi, T., B. J. Hoskins, and H-H. Hsu, 1995: Rossby wave propagation and teleconnection patterns in the austral winter. *J. Atmos. Sci., 52*, 3661-3672.

Bluestein, H. B., 1993: *Synoptic-Dynamic Meteorology in Midlatitudes, Volume II.* Oxford University Press, New York, 594 pp.

Davies, H. C., and A. M. Rossa, 1998: PV frontogenesis and upper tropospheric fronts. *Mon. Wea. Rev.*, *126*, 1528-1539.

Davis, C. A., and K. A. Emanuel, 1991: Potential vorticity diagnostics of cyclogenesis. *Mon. Wea. Rev., 119*, 1929-1953.

Fortune, M., and V. E. Kousky, 1983: Two severe freezes in Brazil: Precursors and synoptic evolution. *Mon. Wea. Rev., 111,* 181-196.

Garreaud, R. D., 2000: Cold air incursions over subtropical and tropical South America: Mean structure and dynamics. *Mon. Wea. Rev., 128*, 2544-2559.

Hoskins, B. J., and F. P. Brotherton, 1972: Atmospheric frontogenesis models: mathematical formulation and solution. *J. Atmos. Sci*., *29*, 11-37.

Hoskins, B. L, M. E. McIntyre, and A. W. Robertson, 1985: On the use and significance of isentropic potential vorticity maps. *Quart. J. Roy. Meteorol. Soc*., *111*, 877-946.

Kalnay, E., M. Kanamitsu, R. Kistler, W. Collins, D. Deaven, L. Gandin, M. Iredell, S. Saha, G. White, J. Woolen, Y. Zhu, M. Chelliah, W. Ebisuzaki, W. Higgins, J. Janoviak, K. C. Mo, C. Ropelewski, J. Wang, A. Leetmaa, R. Reynolds, R. Jenne, and D. Joseph, 1996: The NCEP/NCAR 40-year reanalysis project. *Bull. Amer. Meteorol. Soc.*, *71*, 437-470.

Kousky, V. E., 1979: Frontal influences on Northeast Brazil. *Mon. Wea. Rev.*, *107*, 1140-1153.

Krishnamurti, T. N., M. Tewari, D. R. Chakraborty, J. Marengo, P. L. Silva Dias, and Satyamurty, P., 1999: Downstrearn amplification: A possible precursor to major freeze events over southeastern Brazil. *Wea. Forecasting, 14,* 242-270.

Lupo, R. L., J. J. Nocera, L. F. Bosart, E. G. Hoffman, and D. J. Knight, 2001: South American cold surges: Types composites and case studies. *Mon. Wea. Rev., 129,* 1021-1041.

Marengo, J., A. Cornejo, P. Satyamurty, C. Nobre, and W. Sea, 1997: Cold surges in tropical and extratropical South America: Three strong events in 1994. *Mon. Wea. Rev., 125*, 2759-2786.

Montgomery, M. T., and B. F. Farrel, 1991: Moist surface frontogenesis associated with interior potential vorticity anomalies in a semigeostrophic model. *J. Atmos. Sci., 48*, 343-367.

Muller, G. V. T., R. H. Campagnucci, M. N. Núñez, and M. A. Salles, 2003: Surface circulation associated with frost in the wet pampas. *Int. J. Climatol.*, *23*, 943-962.

Muller, G. V., T. Ambrizzi, and M. N. Núñez, 2005: Mean atmospheric circulation leading to generalized frosts in central southern South America. *Theor. Appl. Climatol., 82*, 95-112.

Muller, G. V., and G. J. Berri, 2006: Atmospheric circulation associated with persistent generalized frosts in central-southern South America. *Mon. Wea. Rev*. (In press).

Nielsen-Gammon, J. W., 2001: A visualization of the global dynamic tropopause. *Bull. Amer. Meteorol. Soc., 82*, 1151-1167.

Pezza, A. B., and T. Ambrizzi, 2005: Dynamical conditions and synoptic tracks associated with different types of cold surges over tropical South America. *Int. J. Climatology*, *25*, 215-241.

Satyamurty, P., and L. F. Mattos, 1989: Climatological lower tropospheric frontogenesis in the midlatitudes due to horizontal deformation and divergence. *Mon.Wea. Rev.,* 117, 1355-1364.

Satyamurty, P., C. A. Nobre, and P. L. Silva Dias, 1998: Tropics: South America. (In) *The Meteorology and Oceanography of the Southern Hemisphere.* Meteorological Monographs No. 49, American Meteorological Society, Boston, 119-139.

Satyamurty, P., J. F. B. Fonseca, M. J. Bottino, M. E. Seluchi, M. C. M. Lourenço, and L. G. Gonçalves, 2002: An early freeze in southern Brazil in April 1999 and its NWP guidance. *Meteorol. Applications, 9,* 113-128.

Vera, C. S. and P. K. Vigliarolo, 2000: A diagnostic study of the cold air outbreaks over South America. *Mon. Wea. Rev., 128,* 3-24.

Vera, C. S., P. K. Vigliarolo, and E. H. Berbery, 2002: Cold season waves over subtropical South America, *Mon. Wea. Rev*., *130*, 684-699.

Figure Legends

Fig. 1. Locator map. ARG: Argentina, URU: Uruguay, PAR: Paraguay, BRA: Brazil. SP: São Paulo state, MG: Minas Gerais state. São Paulo city, the site of the meteorological station, is also shown.

Fig. 2. Trajectories of the highs (a) and lows (b) associated with 12 strong cold surge events in São Paulo from D-7 to D0.

Fig. 3. Surface pressure (hPa) patterns associated with the 12 strong cold surges in São Paulo on D0 (a) to (l). Climatological surface pressure (m), Composite pressure field (n), composite pressure anomaly (o). 1000-500 hPa thickness (geopotential meters) composite is shown in (n). The dates of the cold surge events and the spatial correlations with the composite field are shown below panels (a) to (l). Shading in panel (o) indicates that the anomaly is statistically significant at 95% level.

Fig. 4. Same as in Fig. 3 except for D-1.

Fig. 5. Surface pressure (hPa) and 1000-500 hPa thickness (geopotntial meters) composites (panels a, c, e, g, i, k, m) and surface pressure anomaly composites (panels b, d, f, h, j, l, n) associated with strong cold surges in São Paulo on D-7 through D0 (except D-6). The winter climatology of the surface pressure is shown in panel (o). Shading indicates that the anomaly is statistically significant at 95% level.

Fig. 6. Same as in Fig. 5, except for temperature (K).

Fig. 7. Same as in Fig. 5, except for 500-hPa geopotential (meters).

Fig. 8. Same as in Fig. 5, except for 250-hPa meridional wind component.

Fig. 9. Same as in Fig. 5, except for 925-hPa level frontogenesis function (10^{-10} K m^{-1} s^{-1}). Broken lines indicate frontolysis.

Fig. 10. Same as in Fig. 5, except for isentropic potential vorticity at 325ºK (units: PVU). Broken lines indicate negative values (cyclonic in southern Hemisphere).

Fig. 11. Same as in Fig. 3, except for isentropic potential vorticity at 325ºK (units: PVU). Broken lines indicate negative values.

Fig. 12. Evolution of sea level pressure anomaly (hPa) in the seven-day period prior to the strong cold surge case of 26 July 2005 in São Paulo. Broken lines indicate negative values. Date and the lead time in hours are shown below each panel. The last panel (p) shows the seasonal climatology. Shading indicates that the anomaly is statistically significant.

Fig. 13. Same as in Fig. 12, except for 500-hPa geopotential anomaly (meters).

Fig. 14. Same as in Fig. 12, except for 925-hPa frontogenetic function (10^{-10} K m^{-1} s^{-1}). Broken lines indicate frontolysis. Panel (p) shows July climatology.

Fig. 15. Same as in Fig. 12, except for 925-hPa frontogenetic function anomaly (10^{-10} K m^{-1} s^{-1}). Broken lines indicate frontolysis.

Fig. 16. Same as in Fig. 12, except for isentropic potential vorticity (units: PVU). Broken lines indicate negative values (cyclonic in Southern Hemisphere).

Fig. 17. Same as in Fig. 12, except for isentropic potential vorticity anomaly (units: PVU). Broken lines indicate negative values (cyclonic in Southern Hemisphere).

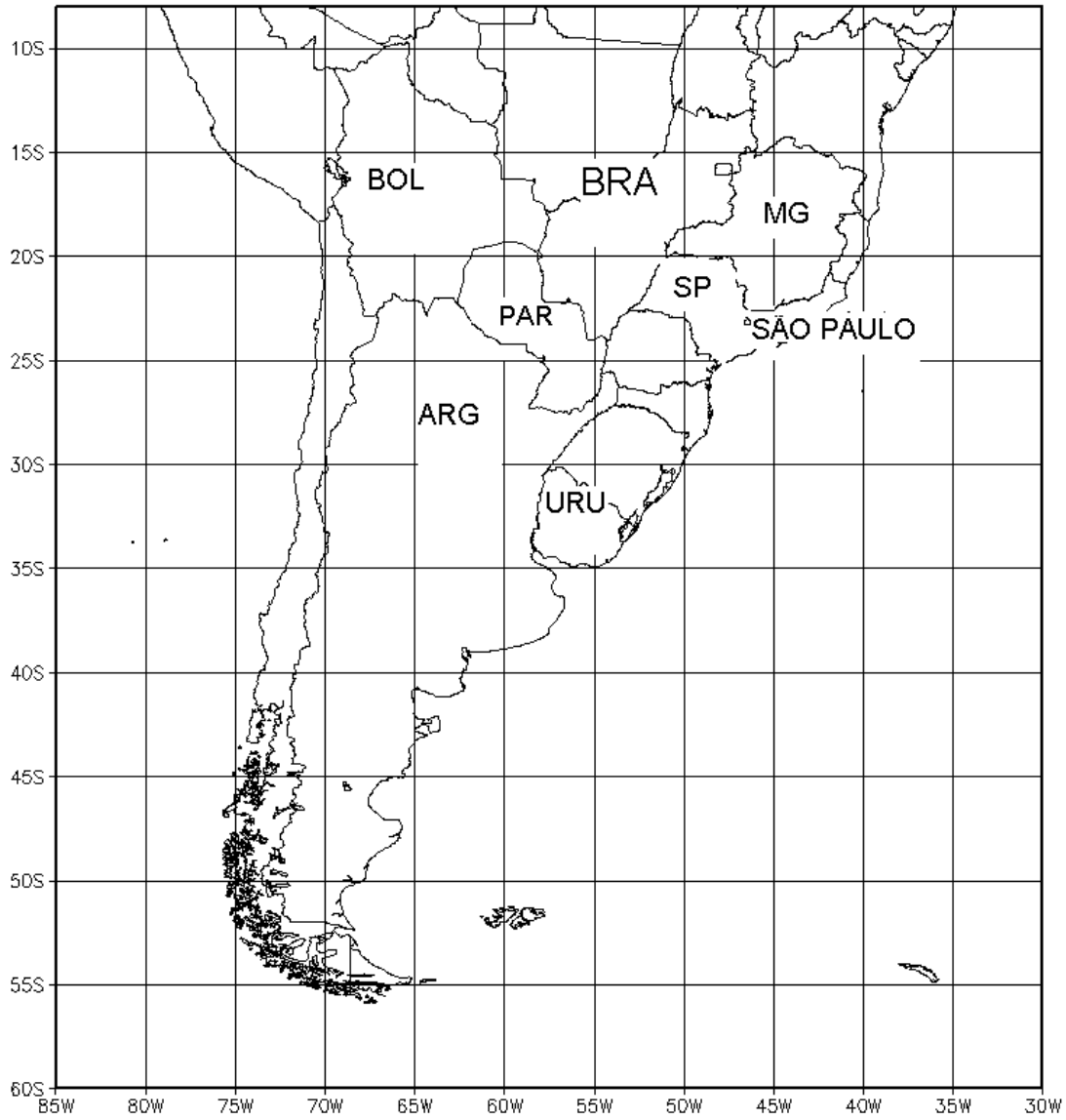
10S
15S
20S
25S
30S
35S
40S
45S
50S
55S
60S
85W
80W
75W
70W
65W
60W
55W
50W
45W
40W
35W
30W
BOL
BRA
MG
SP
PAR
SÃO PAULO
ARG
URU

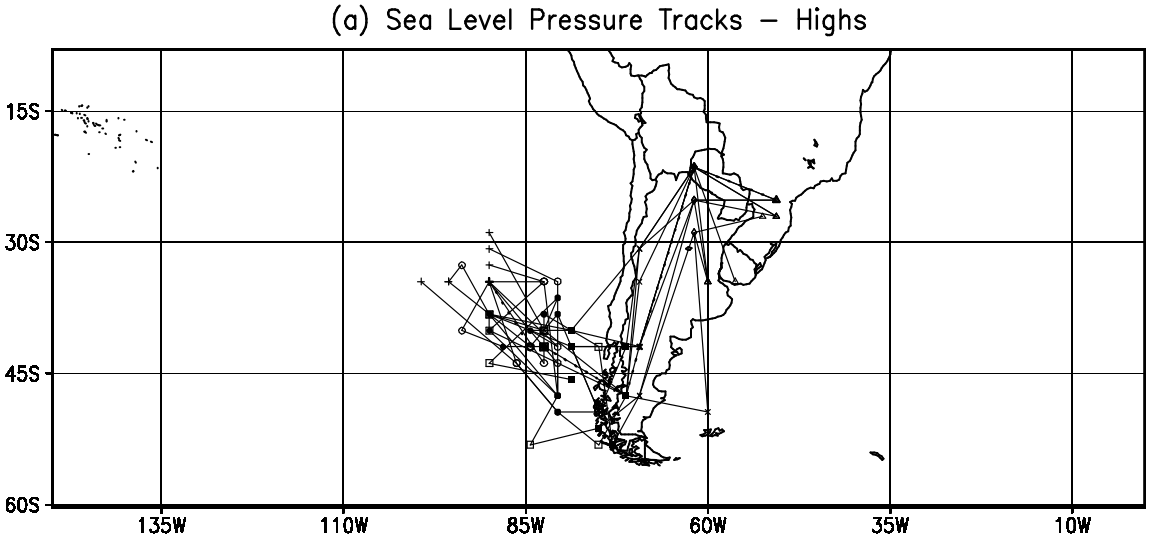
(a) Sea Level Pressure Tracks – Highs
15S
30S
45S
60S
135W
110W
85W
60W
35W
10W

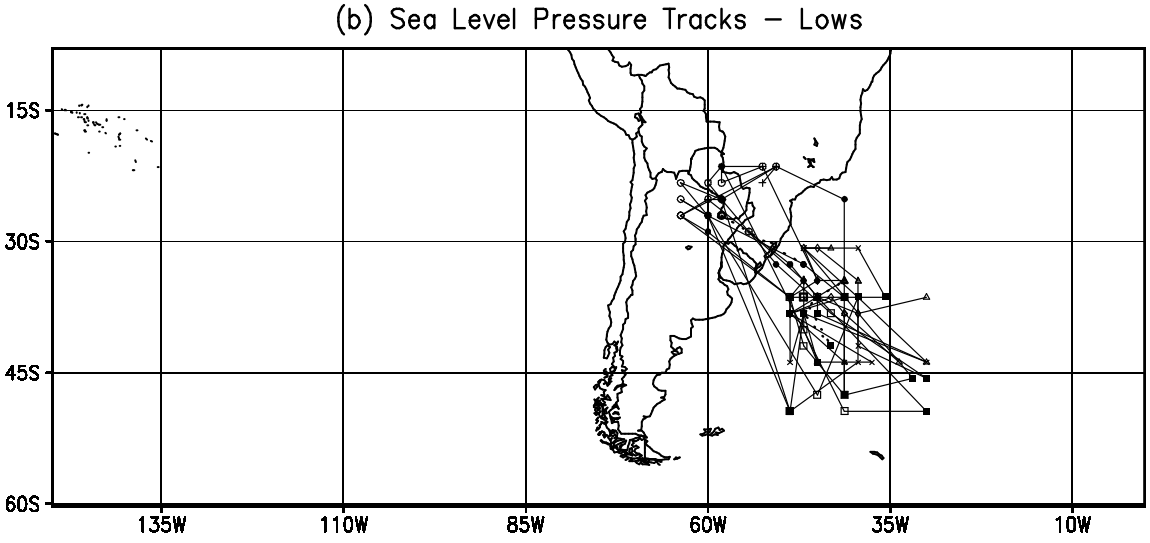
(b) Sea Level Pressure Tracks – Lows
15S
30S
45S
60S
135W
110W
85W
60W
35W
10W

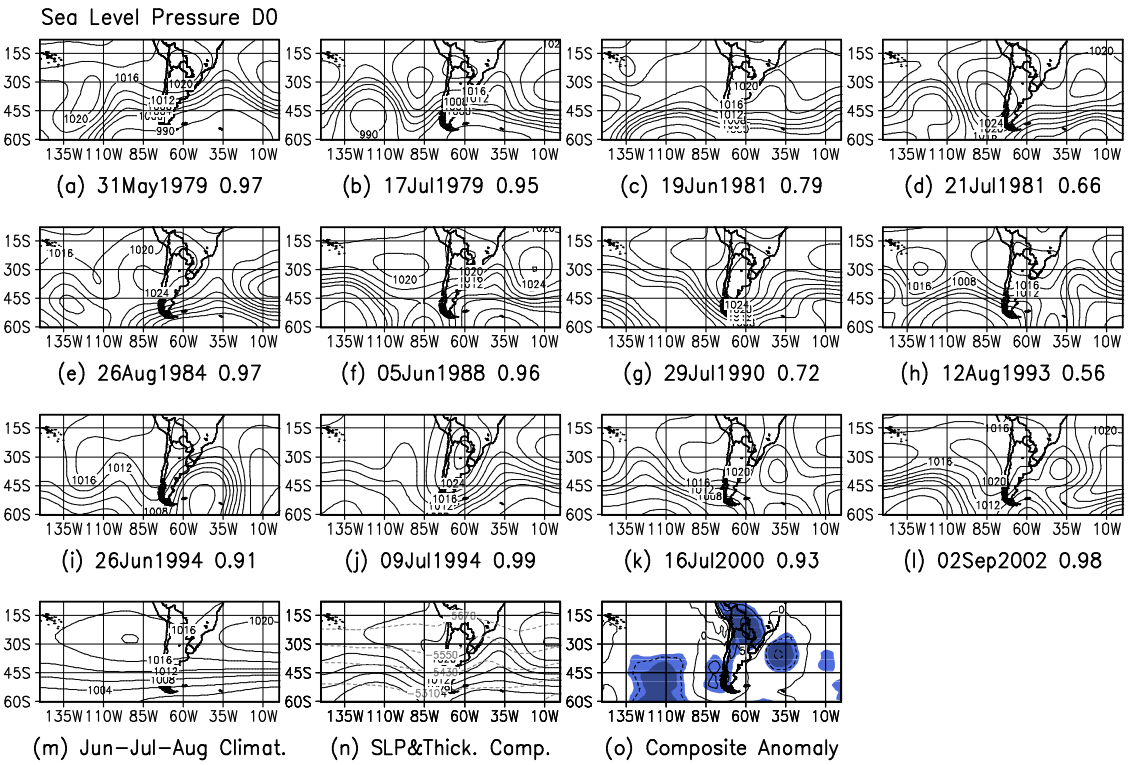
Sea Level Pressure DO
(a) 31May1979 0.97
(b) 17Jul1979 0.95
(c) 19Jun1981 0.79
(d) 21Jul1981 0.66
(e) 26Aug1984 0.97
(f) 05Jun1988 0.96
(g) 29Jul1990 0.72
(h) 12Aug1993 0.56
(i) 26Jun1994 0.91
(j) 09Jul1994 0.99
(k) 16Jul2000 0.93
(l) 02Sep2002 0.98
(m) Jun–Jul–Aug Climat.
(n) SLP&Thick. Comp.
(o) Composite Anomaly
15S
30S
45S
60S
135W 110W 85W 60W 35W 10W

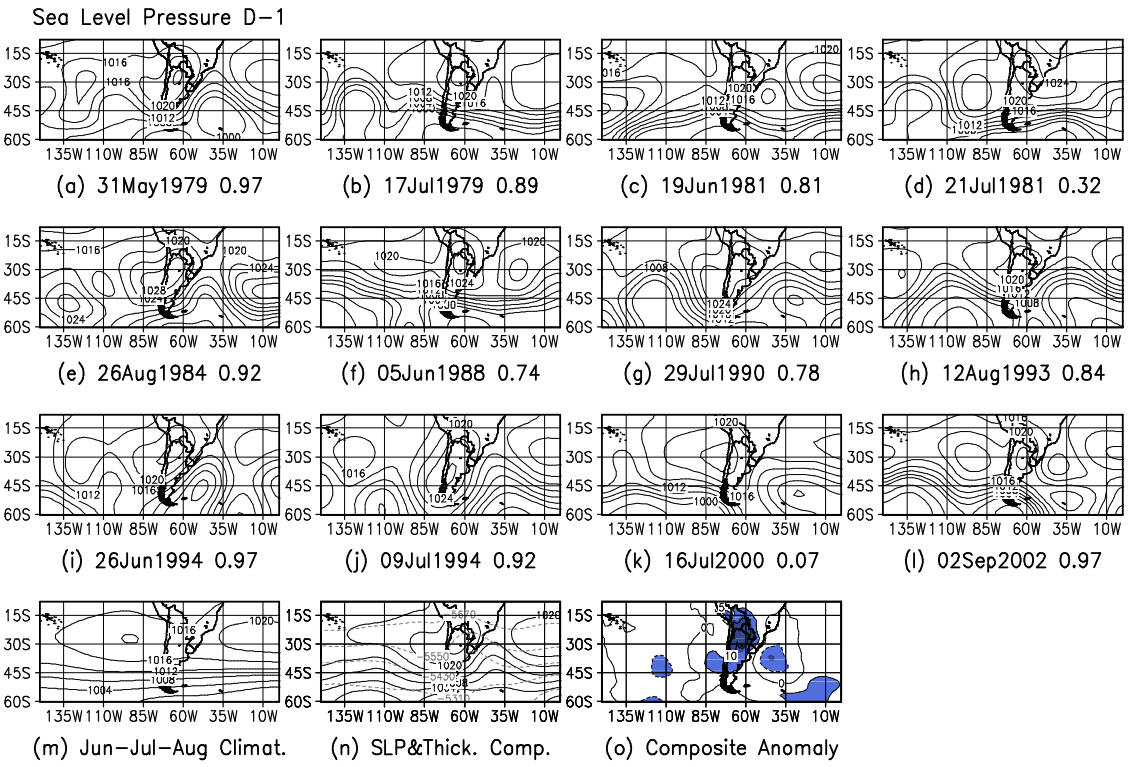
Sea Level Pressure D−1
(a) 31May1979 0.97
(b) 17Jul1979 0.89
(c) 19Jun1981 0.81
(d) 21Jul1981 0.32
(e) 26Aug1984 0.92
(f) 05Jun1988 0.74
(g) 29Jul1990 0.78
(h) 12Aug1993 0.84
(i) 26Jun1994 0.97
(j) 09Jul1994 0.92
(k) 16Jul2000 0.07
(l) 02Sep2002 0.97
(m) Jun−Jul−Aug Climat.
(n) SLP&Thick. Comp.
(o) Composite Anomaly
15S
30S
45S
60S
135W 110W 85W 60W 35W 10W

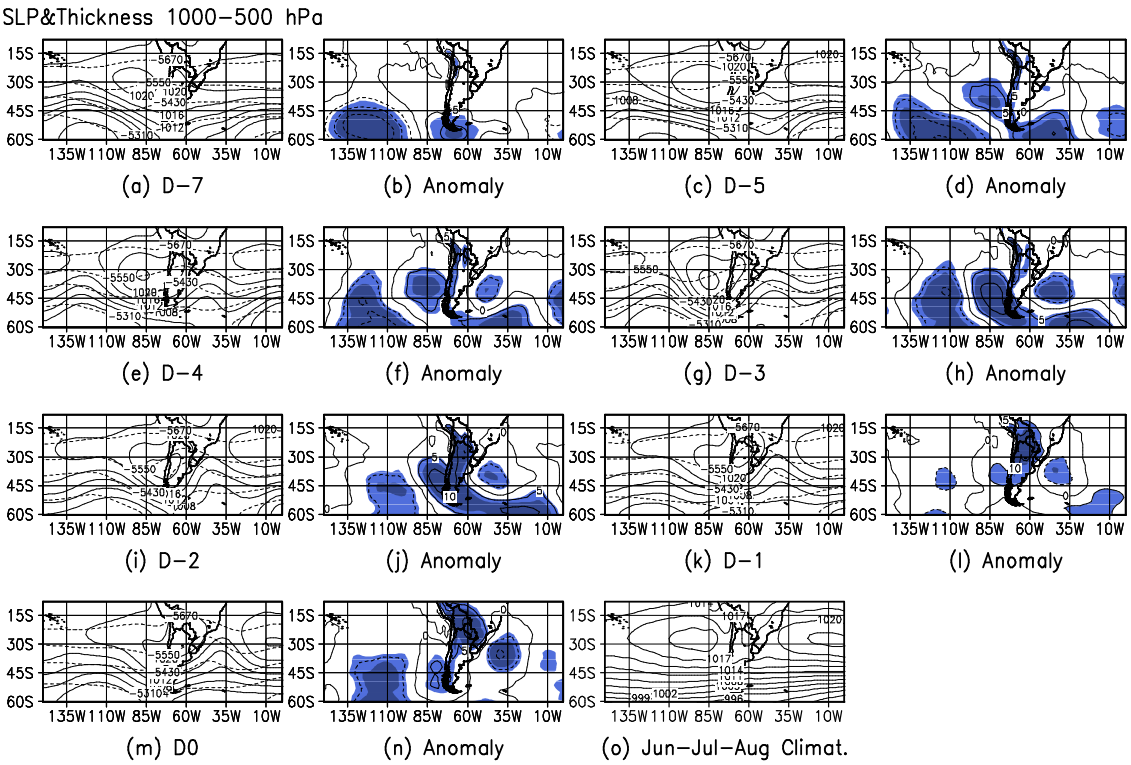
SLP&Thickness 1000−500 hPa
(a) D−7
(b) Anomaly
(c) D−5
(d) Anomaly
(e) D−4
(f) Anomaly
(g) D−3
(h) Anomaly
(i) D−2
(j) Anomaly
(k) D−1
(l) Anomaly
(m) D0
(n) Anomaly
(o) Jun−Jul−Aug Climat.
15S
30S
45S
60S
135W 110W 85W 60W 35W 10W

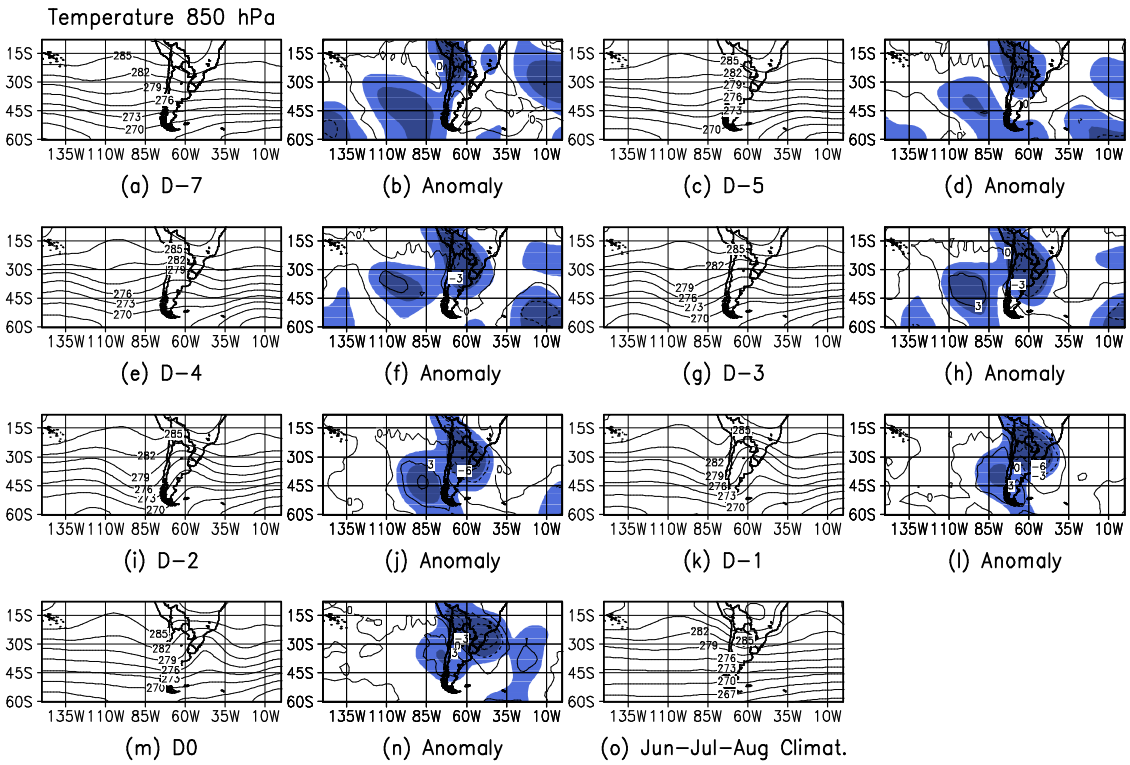
Temperature 850 hPa
(a) D−7
(b) Anomaly
(c) D−5
(d) Anomaly
(e) D−4
(f) Anomaly
(g) D−3
(h) Anomaly
(i) D−2
(j) Anomaly
(k) D−1
(l) Anomaly
(m) D0
(n) Anomaly
(o) Jun−Jul−Aug Climat.

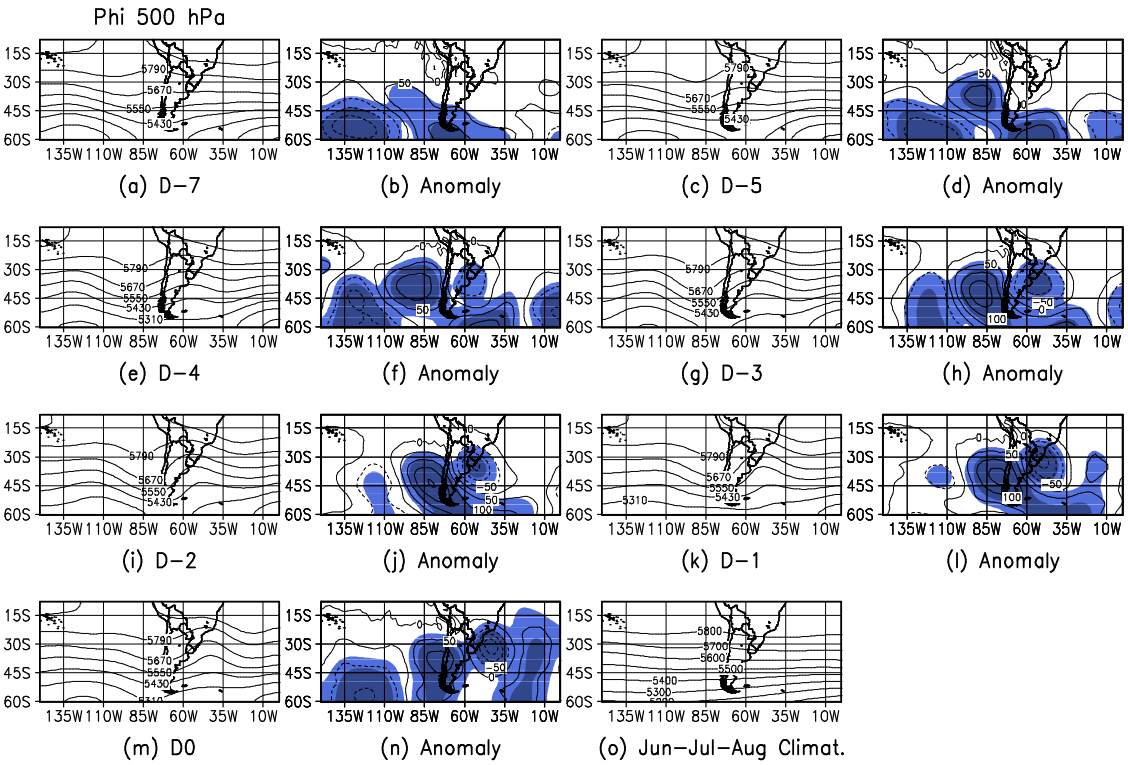
Phi 500 hPa
(a) D−7
(b) Anomaly
(c) D−5
(d) Anomaly
(e) D−4
(f) Anomaly
(g) D−3
(h) Anomaly
(i) D−2
(j) Anomaly
(k) D−1
(l) Anomaly
(m) D0
(n) Anomaly
(o) Jun−Jul−Aug Climat.

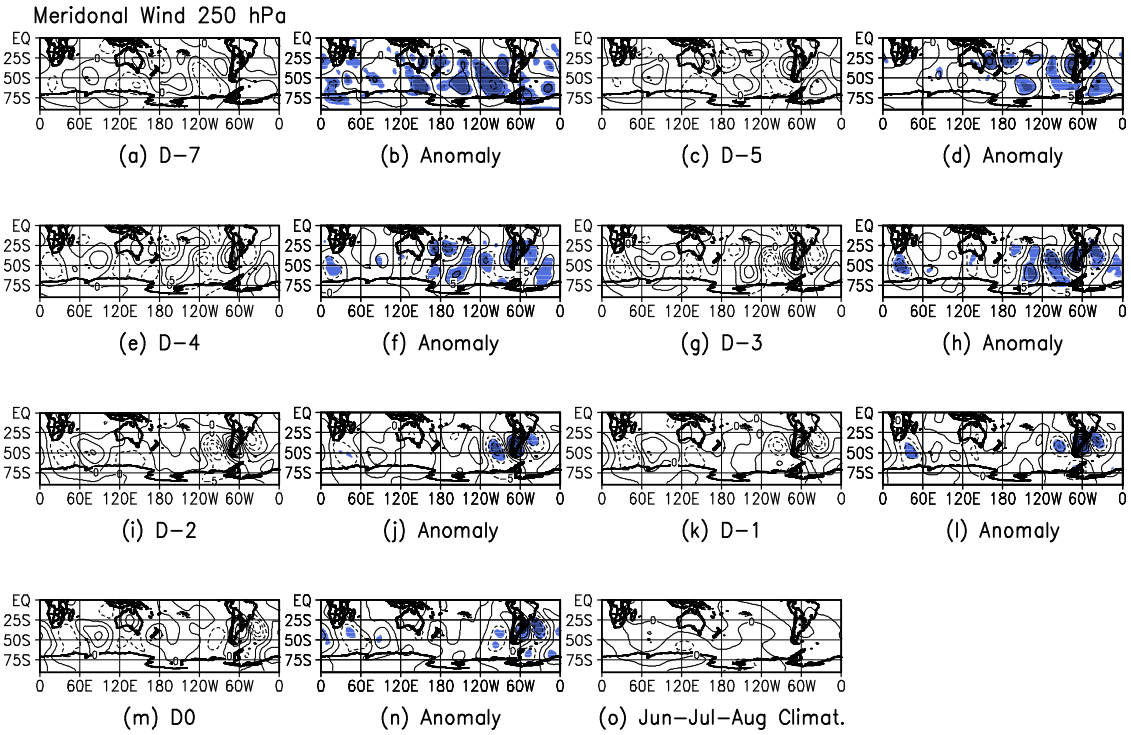
Meridonal Wind 250 hPa
EQ
25S
50S
75S
0 60E 120E 180 120W 60W 0
(a) D−7
(b) Anomaly
(c) D−5
(d) Anomaly
(e) D−4
(f) Anomaly
(g) D−3
(h) Anomaly
(i) D−2
(j) Anomaly
(k) D−1
(l) Anomaly
(m) D0
(n) Anomaly
(o) Jun−Jul−Aug Climat.

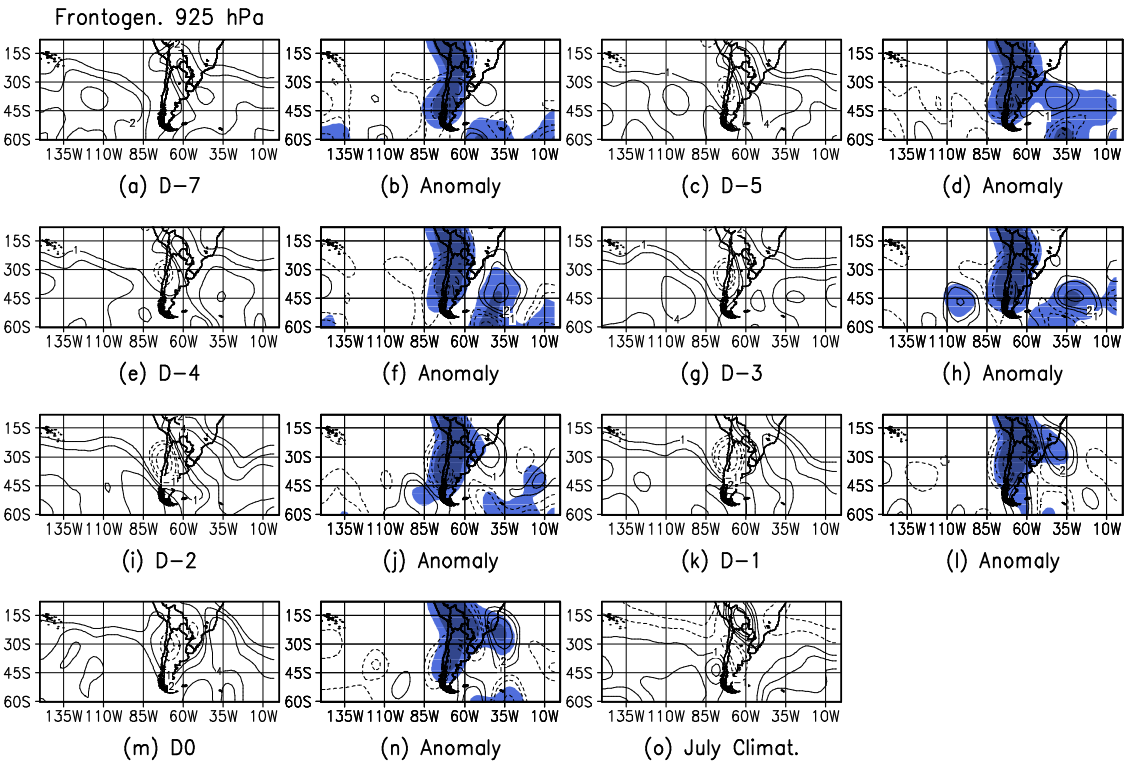
Frontogen. 925 hPa
15S
30S
45S
60S
135W 110W 85W 60W 35W 10W
(a) D−7
(b) Anomaly
(c) D−5
(d) Anomaly
(e) D−4
(f) Anomaly
(g) D−3
(h) Anomaly
(i) D−2
(j) Anomaly
(k) D−1
(l) Anomaly
(m) D0
(n) Anomaly
(o) July Climat.

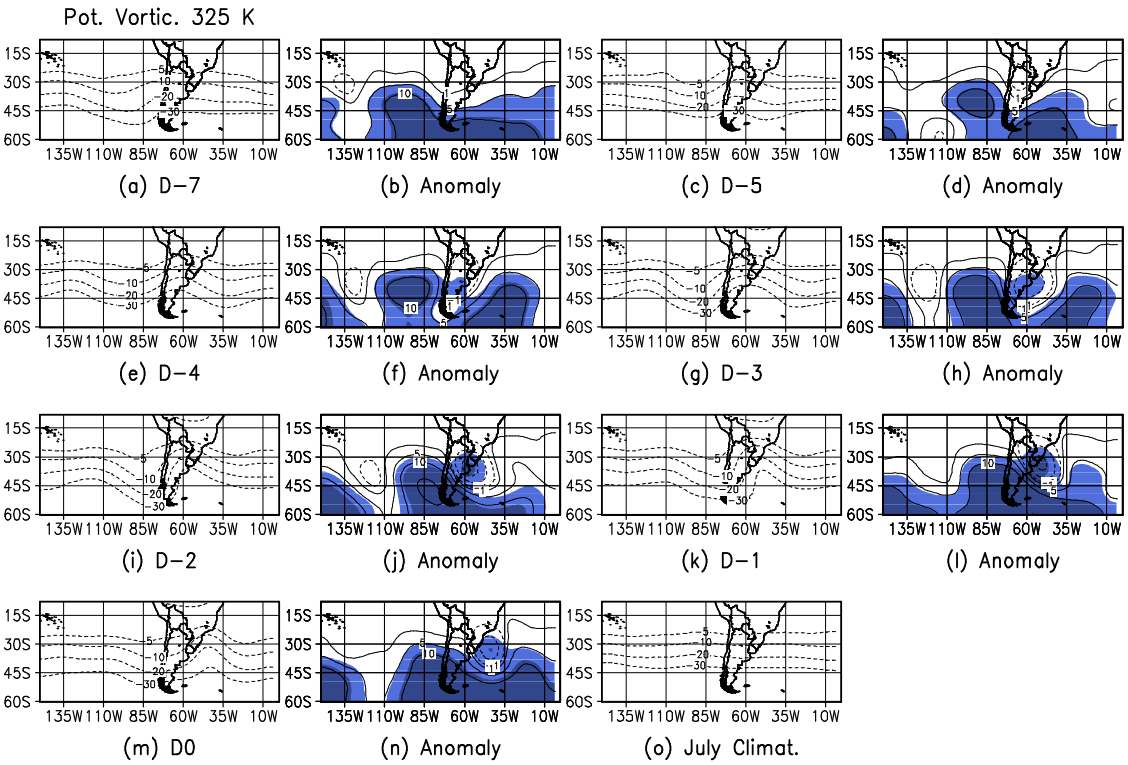
Pot. Vortic. 325 K
(a) D−7
(b) Anomaly
(c) D−5
(d) Anomaly
(e) D−4
(f) Anomaly
(g) D−3
(h) Anomaly
(i) D−2
(j) Anomaly
(k) D−1
(l) Anomaly
(m) D0
(n) Anomaly
(o) July Climat.
15S
30S
45S
60S
135W 110W 85W 60W 35W 10W

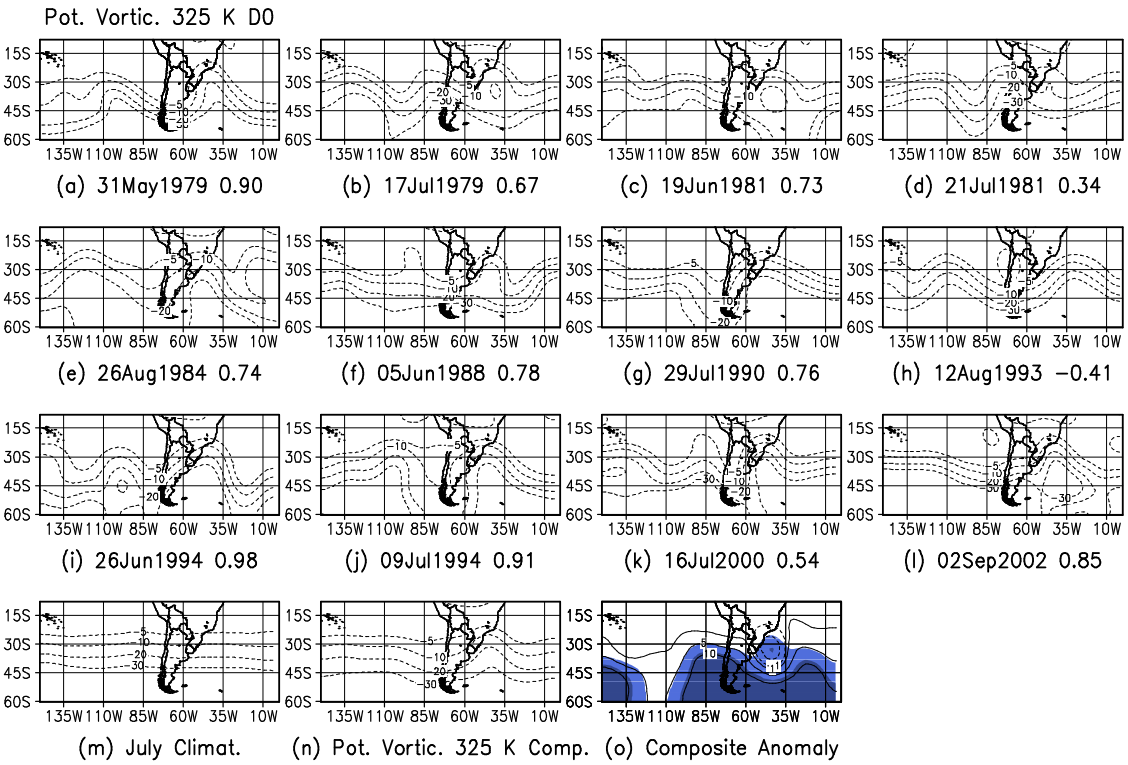
Pot. Vortic. 325 K D0
15S
30S
45S
60S
135W 110W 85W 60W 35W 10W
(a) 31May1979 0.90
(b) 17Jul1979 0.67
(c) 19Jun1981 0.73
(d) 21Jul1981 0.34
(e) 26Aug1984 0.74
(f) 05Jun1988 0.78
(g) 29Jul1990 0.76
(h) 12Aug1993 −0.41
(i) 26Jun1994 0.98
(j) 09Jul1994 0.91
(k) 16Jul2000 0.54
(l) 02Sep2002 0.85
(m) July Climat.
(n) Pot. Vortic. 325 K Comp.
(o) Composite Anomaly

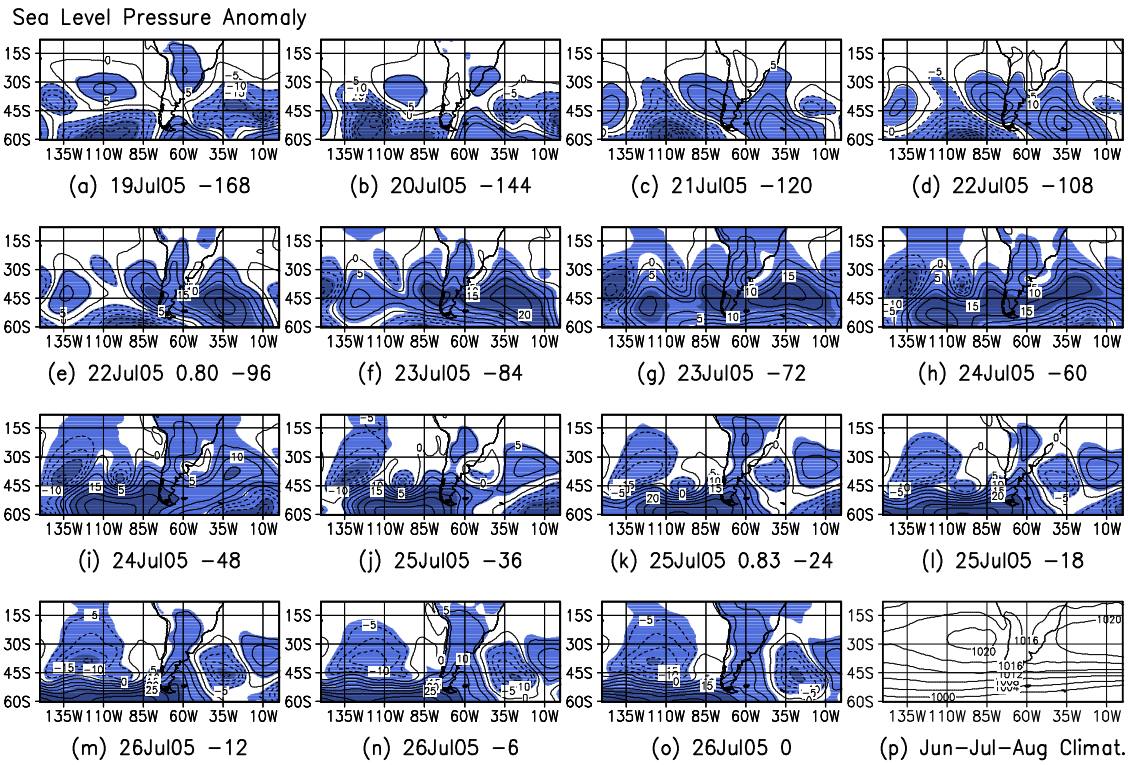
Sea Level Pressure Anomaly
15S
30S
45S
60S
135W 110W 85W 60W 35W 10W
(a) 19Jul05 −168
(b) 20Jul05 −144
(c) 21Jul05 −120
(d) 22Jul05 −108
(e) 22Jul05 0.80 −96
(f) 23Jul05 −84
(g) 23Jul05 −72
(h) 24Jul05 −60
(i) 24Jul05 −48
(j) 25Jul05 −36
(k) 25Jul05 0.83 −24
(l) 25Jul05 −18
(m) 26Jul05 −12
(n) 26Jul05 −6
(o) 26Jul05 0
(p) Jun−Jul−Aug Climat.

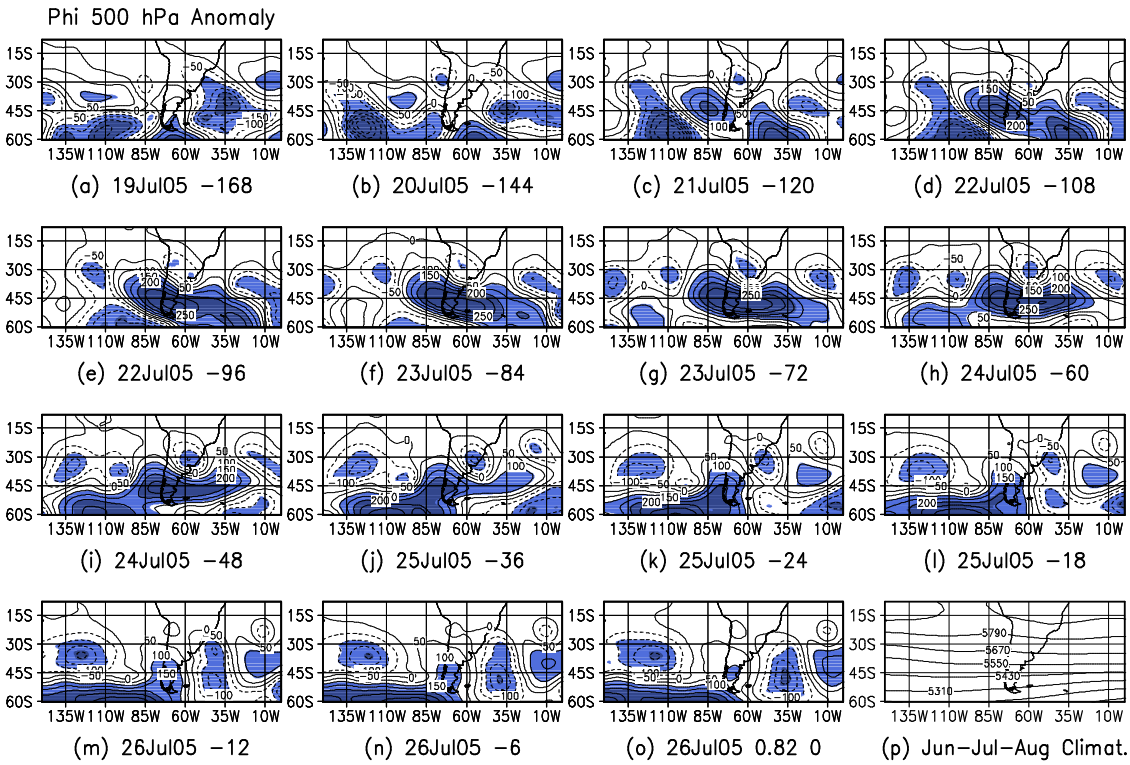
Phi 500 hPa Anomaly
(a) 19Jul05 −168
(b) 20Jul05 −144
(c) 21Jul05 −120
(d) 22Jul05 −108
(e) 22Jul05 −96
(f) 23Jul05 −84
(g) 23Jul05 −72
(h) 24Jul05 −60
(i) 24Jul05 −48
(j) 25Jul05 −36
(k) 25Jul05 −24
(l) 25Jul05 −18
(m) 26Jul05 −12
(n) 26Jul05 −6
(o) 26Jul05 0.82 0
(p) Jun−Jul−Aug Climat.
15S
30S
45S
60S
135W 110W 85W 60W 35W 10W

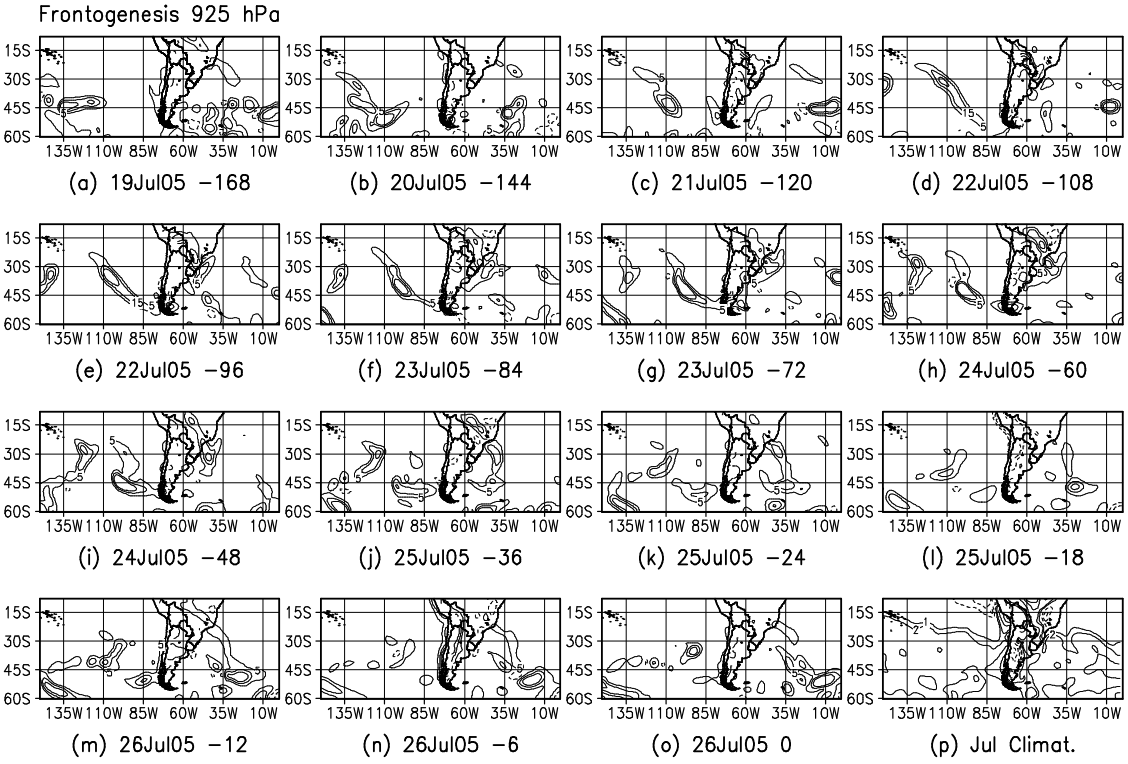
Frontogenesis 925 hPa
15S
30S
45S
60S
135W 110W 85W 60W 35W 10W
(a) 19Jul05 −168
(b) 20Jul05 −144
(c) 21Jul05 −120
(d) 22Jul05 −108
(e) 22Jul05 −96
(f) 23Jul05 −84
(g) 23Jul05 −72
(h) 24Jul05 −60
(i) 24Jul05 −48
(j) 25Jul05 −36
(k) 25Jul05 −24
(l) 25Jul05 −18
(m) 26Jul05 −12
(n) 26Jul05 −6
(o) 26Jul05 0
(p) Jul Climat.

Frontogen. 925 hPa Anomaly

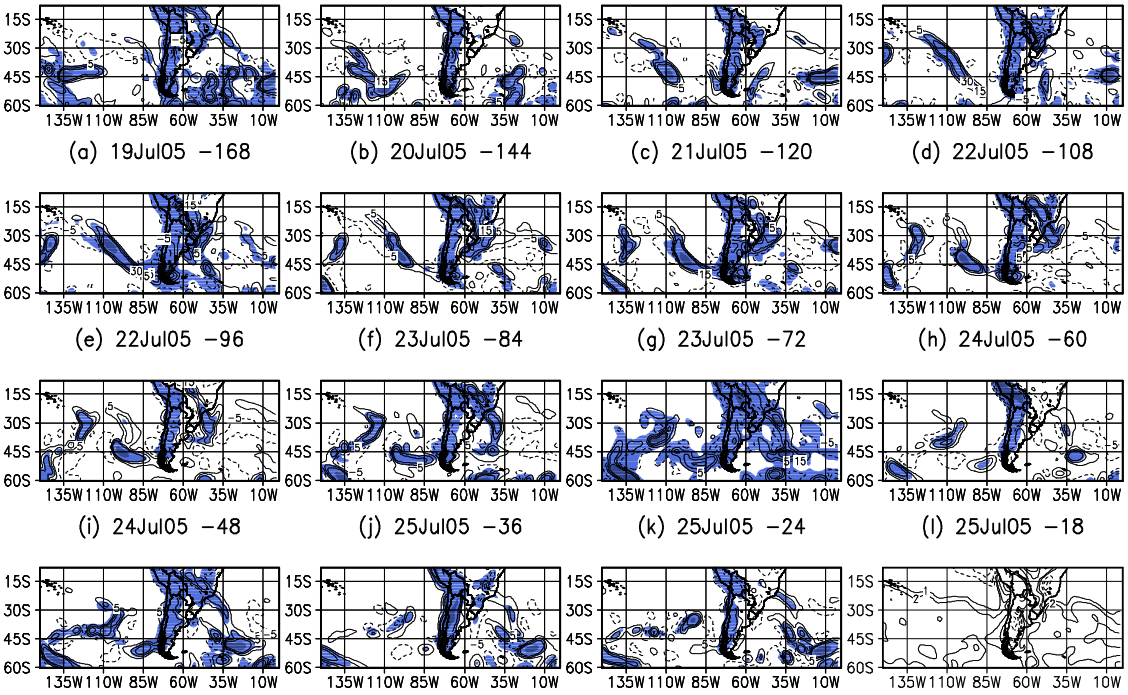

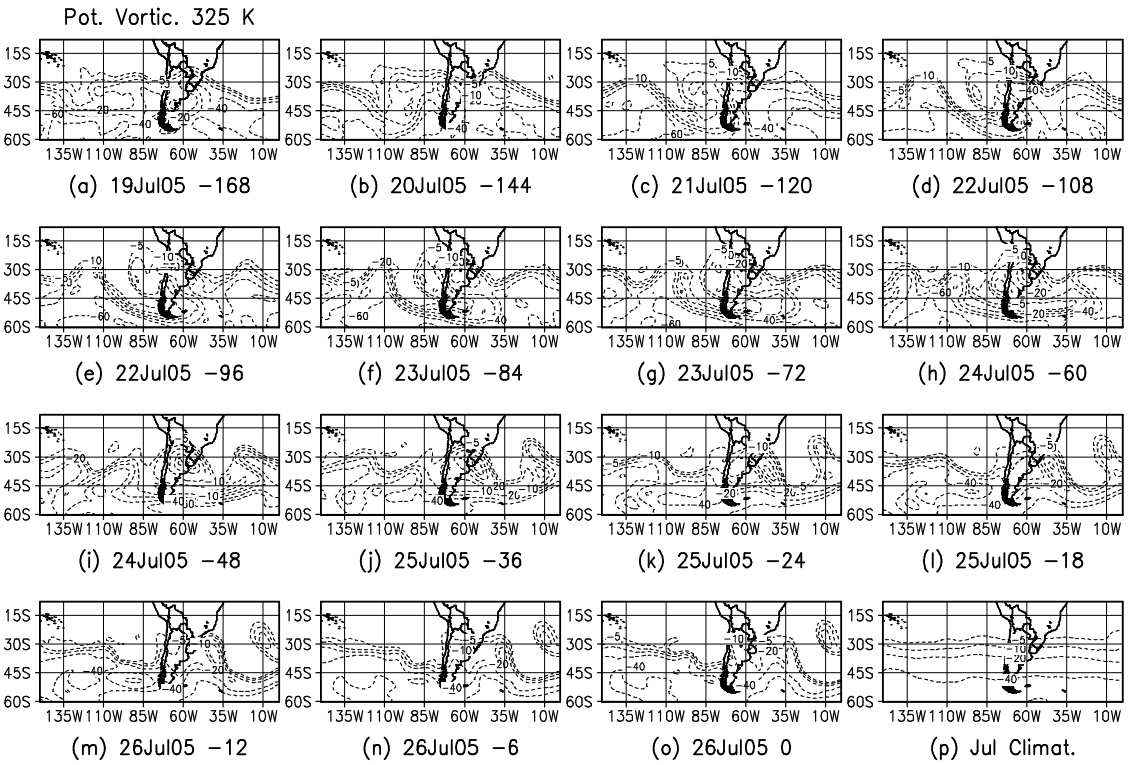
Pot. Vortic. 325 K
15S
30S
45S
60S
135W 110W 85W 60W 35W 10W
(a) 19Jul05 −168
(b) 20Jul05 −144
(c) 21Jul05 −120
(d) 22Jul05 −108
(e) 22Jul05 −96
(f) 23Jul05 −84
(g) 23Jul05 −72
(h) 24Jul05 −60
(i) 24Jul05 −48
(j) 25Jul05 −36
(k) 25Jul05 −24
(l) 25Jul05 −18
(m) 26Jul05 −12
(n) 26Jul05 −6
(o) 26Jul05 0
(p) Jul Climat.

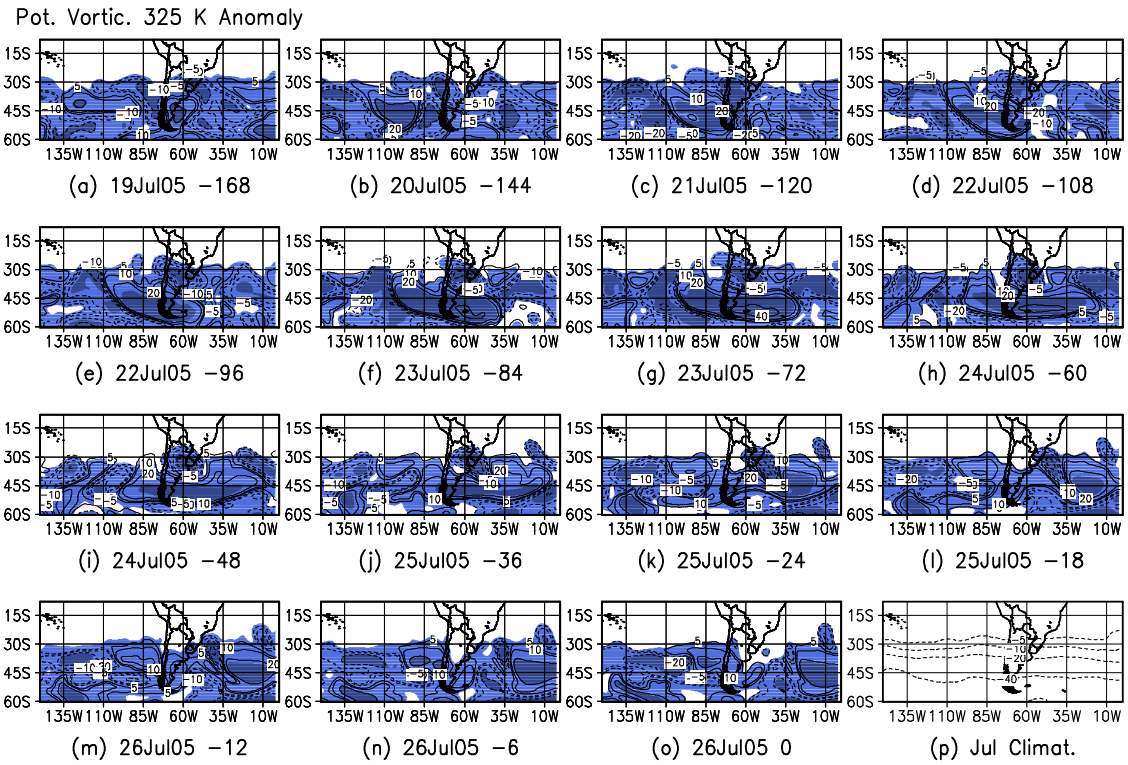
Pot. Vortic. 325 K Anomaly
15S
30S
45S
60S
135W 110W 85W 60W 35W 10W
(a) 19Jul05 −168
(b) 20Jul05 −144
(c) 21Jul05 −120
(d) 22Jul05 −108
(e) 22Jul05 −96
(f) 23Jul05 −84
(g) 23Jul05 −72
(h) 24Jul05 −60
(i) 24Jul05 −48
(j) 25Jul05 −36
(k) 25Jul05 −24
(l) 25Jul05 −18
(m) 26Jul05 −12
(n) 26Jul05 −6
(o) 26Jul05 0
(p) Jul Climat.